BRIEF COMMUNICATION
https://doi.org/10.1038/s41587-020-0500-9
nature biotechnology

Plants with genetically encoded autoluminescence

Tatiana Mitiouchkina[1,2,10], Alexander S. Mishin[1,2,10], Louisa Gonzalez Somermeyer[3,10], Nadezhda M. Markina[1,2,10], Tatiana V. Chepurnyh[1,2], Elena B. Guglya[2,4], Tatiana A. Karataeva[1,2], Kseniia A. Palkina[1,2], Ekaterina S. Shakhova[1,2], Liliia I. Fakhranurova[1,2], Sofia V. Chekova[1], Aleksandra S. Tsarkova[1,2,5], Yaroslav V. Golubev[4], Vadim V. Negrebetsky[4], Sergey A. Dolgushin[6], Pavel V. Shalaev[6], Dmitry Shlykov[2], Olesya A. Melnik[1,2], Victoria O. Shipunova[2], Sergey M. Deyev[2], Andrey I. Bubyrev[2], Alexander S. Pushin[1,2], Vladimir V. Choob[7], Sergey V. Dolgov[2], Fyodor A. Kondrashov[3], Ilia V. Yampolsky[1,2,4,10] ✉ and Karen S. Sarkisyan[1,2,8,9,10] ✉

Autoluminescent plants engineered to express a bacterial bioluminescence gene cluster in plastids have not been widely adopted because of low light output. We engineered tobacco plants with a fungal bioluminescence system that converts caffeic acid (present in all plants) into luciferin and report self-sustained luminescence that is visible to the naked eye. Our findings could underpin development of a suite of imaging tools for plants.

Bioluminescent reporters have not been broadly applied in plants because exogenous addition of luciferin is expensive and can be toxic. Although bacterial bioluminescence genes can be targeted to plastids to engineer autoluminescence, it is technically cumbersome and fails to produce sufficient light[1]. The caffeic acid cycle, which is a metabolic pathway responsible for luminescence in fungi, was recently characterized[2]. We report light emission in *Nicotiana tabacum* and *Nicotiana benthamiana* plants without the addition of any exogenous substrate by engineering fungal bioluminescence genes into the plant nuclear genome.

Caffeic acid is an intermediate in the phenylpropanoid pathway, which produces lignin and other metabolites in vascular plants. We reasoned that it might be feasible to integrate the fungal caffeic acid cycle into plant metabolism. Moreover, the green luminescence produced by the caffeic acid cycle fits well with the optical transparency window of pigmented plant tissues (Fig. 1a). Although caffeic acid is not native to animals, autonomous luminescence could also be enabled in animals by including two additional enzymes needed for its biosynthesis from tyrosine—tyrosine ammonia lyase and coumarate 3-hydroxylase—or their functional equivalents (Fig. 1b and Supplementary Fig. 1)[3].

We engineered autonomously glowing *N. tabacum* plants by random-site genome integration using *Agrobacterium*-mediated transformation of DNA cassettes comprising codon-optimized versions of four *Neonothopanus nambi* bioluminescence genes[2]: *nnluz* (luciferase), *nnhisps* (hispidin synthase), *nnh3h* (hispidin-3-hydroxylase) and *nncph* (caffeoyl pyruvate hydrolase) (Fig. 1, Methods, Supplementary Fig. 2 and Supplementary Note 1). Fifteen independently obtained plant lines had confirmed genome integration events. The overall phenotype, chlorophyll and carotenoid content, flowering time and seed germination did not differ from wild-type tobacco in the greenhouse, with the exception of a 12% increase in median height of transgenic plants (Supplementary Fig. 3 and Supplementary Note 2). This suggests that, unlike expression of bacterial bioluminescence system[1], expression of caffeic acid cycle is not toxic in plants and does not impose an obvious burden on plant growth, at least in the greenhouse. Light emission at all developmental stages was visible to the naked eye, with intensity from the flowers reaching 10^{10} photons per minute (Supplementary Table 1). This level of brightness allowed us to capture detailed images on consumer-grade cameras with exposure times of 0.5–30 s, providing similar quality to that of more expensive luminescence imaging equipment (Fig. 2 and Supplementary Figs. 3–8).

To identify metabolites that might limit light emission, we infused leaves of glowing plants with luciferin or its precursors. We found that bright luminescence developed instantly after injections of luciferin or hispidin, whereas lower intensity was produced more slowly if leaves were supplemented with caffeic acid (Supplementary Video 1). Because engineered *N. tabacum* lines did not retain infused exogenous precursors at the injection site, we created a glowing line of *N. benthamiana*. In evaluation of all-but-one mixtures of hispidin precursors, caffeic acid produced increased luminescence, whereas malonyl-CoA, CoA or ATP, added individually or as a mixture, did not (Supplementary Note 3 and Supplementary Fig. 9). Taken together, these experiments suggest that caffeic acid limits hispidin biosynthesis (Supplementary Note 4 and Supplementary Video 1).

Consistent with a link between caffeic acid availability and luminescence intensity, the distribution of luminescence resembled reported expression patterns of enzymes involved in the phenylpropanoid pathway[4]. During seed germination, there was increased luminescence at the tips of cotyledons and roots (Fig. 2a and Supplementary Video 2). Roots also glowed brightly at branching points (Fig. 2d), often hours before visible evidence of lateral root

[1]Planta LLC, Moscow, Russia. [2]Shemyakin-Ovchinnikov Institute of Bioorganic Chemistry, Russian Academy of Sciences, Moscow, Russia. [3]Institute of Science and Technology Austria, Klosterneuburg, Austria. [4]Pirogov Russian National Research Medical University, Moscow, Russia. [5]Institute of Biophysics, Krasnoyarsk Science Center of the Siberian Branch of the Russian Academy of Sciences, Krasnoyarsk, Russia. [6]Aivok LLC, Zelenograd, Moscow, Russia. [7]Botanical Garden of Lomonosov Moscow State University, Moscow, Russia. [8]Synthetic Biology Group, MRC London Institute of Medical Sciences, London, UK. [9]Institute of Clinical Sciences, Faculty of Medicine and Imperial College Centre for Synthetic Biology, Imperial College London, London, UK. [10]These authors contributed equally: Tatiana Mitiouchkina, Alexander S. Mishin, Louisa Gonzalez Somermeyer, Nadezhda M. Markina, Ilia V. Yampolsky, Karen S. Sarkisyan. ✉e-mail: ivyamp@gmail.com; karen@planta.bio

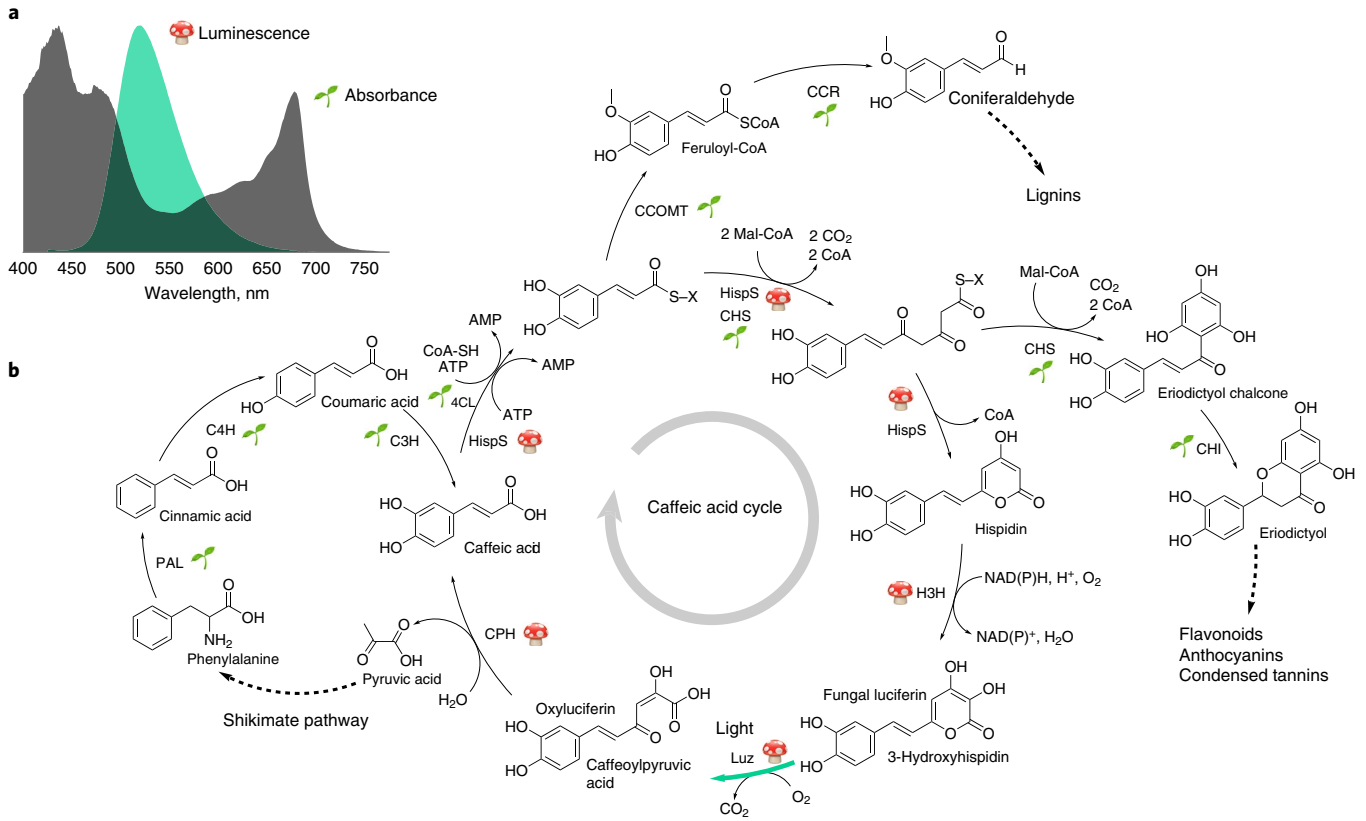

Fig. 1 | Fungal bioluminescence system. a, Spectrum of fungal bioluminescence (*N. nambi*, in green) overlaid onto the absorbance spectrum of plant leaves (*N. tabacum*, in dark gray). **b**, The caffeic acid cycle shares metabolites with some of the major plant biosynthetic pathways. The fungal or plant origin of enzymes is indicated with mushroom and plantlet symbols, respectively. 4CL, 4-coumarate:CoA ligase; C3H, *p*-coumaric acid 3-hydroxylase; C4H, cinnamic acid 4-hydroxylase; CCOMT, caffeoyl-CoA 3-*O*-methyltransferase; CCR, cinnamoyl-CoA reductase; CHI, chalcone isomerase; CHS, chalcone synthase; CPH, putative caffeoyl pyruvate hydrolase; H3H, hispidin-3-hydroxylase; HispS, hispidin synthase; Luz, luciferase; PAL, phenylalanine ammonia-lyase. Absorbance spectrum of leaf is representative of experiment performed on three leaves. The luminescence spectrum is rendered from a data set published in ref. [3].

initiation (Supplementary Videos 3 and 4). As plants developed, luminescence increased at the transition zone between the root and the stem. Young shoots were brightest at the terminal and axillary buds and at the upper part of the stem; older parts of the shoot dimmed as plants matured (Supplementary Video 5). Flowers produced the most luminescence (Fig. 2c,e, Supplementary Fig. 10 and Supplementary Video 6).

Increased light emission under conditions known to activate production of phenylpropanoids was observed using time-lapse luminescent imaging. Moreover, the spatial and temporal patterns of luminescence of tobacco plants were characterized (Supplementary Notes 5–7). In injured leaves[5,6], we observed a sustained increase in light emission at the injury site. We also discerned luminescence spreading from an injury site via small veins at approximately 2 µm s^{-1} (Supplementary Fig. 11 and Supplementary Video 7). Apical shoot removal[7] resulted in sustained bright luminescence in lateral shoots proximal to the cut site (Supplementary Fig. 12 and Supplementary Video 8). Aging leaves, reported to have gradually reducing caffeic acid content until late senescence[8], generally exhibited decreased light emission. Nevertheless, some leaves displayed waves of intense light emission during the final stages of senescence (Supplementary Video 5), possibly reflecting age-related nutrient remobilization[9,10]. Finally, plants treated with methyl jasmonate[11,12] or ripe banana skin (which emits ethylene, among other compounds)[13] responded with massively increased luminescence throughout the plant (Supplementary Fig. 13a,b).

We have established the feasibility of using fungal bioluminescence genes to produce glowing plants that are at least an order of magnitude brighter than was previously achieved using a bacterial bioluminescence system (Supplementary Table 1 and Supplementary Figs. 6 and 7)[1]. By enabling autonomous light emission, dynamic processes in plants can be monitored, including development and pathogenesis, responses to environmental conditions and effects of chemical treatment. Screening methods should also be enabled by the simplicity and efficiency of acquiring luminescent data. By removing the need for exogenous addition of luciferin or other substrates, these luminescent capabilities should be particularly useful for experiments with plants grown in the soil.

Online content

Any methods, additional references, Nature Research reporting summaries, source data, extended data, supplementary information, acknowledgements, peer review information; details of author contributions and competing interests; and statements of data and code availability are available at https://doi.org/10.1038/s41587-020-0500-9.

Received: 24 July 2019; Accepted: 26 March 2020;
Published online: 27 April 2020

Fig. 2 | Bioluminescent plants during development. Light emission from *N. tabacum* plants at germination (**a**), vegetative (**b**) and flowering (**c**) stages; light emission from roots (**d**) and cross section of flowers (**e**). Photos were captured on a Sony Alpha ILCE-7M3 camera (Methods). The 110 seedlings depicted in **a** are representative of three independent experiments. Images of plants in vegetative (**b**, 3 weeks) and flowering (**c**, 8 weeks) stages, as well as individual flowers (**e**) are representative of 100 plants followed from in vitro to flowering in four separate experiments. The age of plants is stated relative to transfer from in vitro to the greenhouse. The image of roots of an individual plant depicted in **d** is representative of three independent imaging experiments on six plants.

References

1. Krichevsky, A., Meyers, B., Vainstein, A., Maliga, P. & Citovsky, V. *PLoS ONE* **5**, e15461 (2010).
2. Kotlobay, A. A. et al. *Proc. Natl Acad. Sci. USA* **115**, 12728–12732 (2018).
3. Yan, Y. & Lin, Y. Biosynthesis of caffeic acid and caffeic acid derivatives by recombinant microorganisms. US patent 8809028B2 (2012).
4. Kawamata, S. et al. *Plant Cell Physiol.* **38**, 792–803 (1997).
5. Gaquerel, E., Gulati, J. & Baldwin, I. T. *Plant J.* **79**, 679–692 (2014).
6. Toyota, M. et al. *Science* **361**, 1112–1115 (2018).
7. Singh, S. K. et al. *Sci. Rep.* **5**, 18148 (2015).
8. Li, L. et al. *Sci. Rep.* **6**, 37976 (2016).
9. Li, W. et al. *Sci. Rep.* **7**, 12126 (2017).
10. Woo, H. R., Kim, H. J., Nam, H. G. & Lim, P. O. *J. Cell Sci.* **126**, 4823–4833 (2013).
11. Pauwels, L. et al. *Proc. Natl Acad. Sci. USA* **105**, 1380–1385 (2008).
12. Bernards, M. A. & Båstrup-Spohr, L. *Induced Plant Resistance to Herbivory* (Springer, 2008).
13. Singh, R., Rastogi, S. & Dwivedi, U. N. *Compr. Rev. Food Sci. Food Saf.* **9**, 398–416 (2010).

Methods

Assembly of plasmids for plant transformation. Coding sequences of the *nnluz*, *nnhisps*, *nnh3h* and *nncph* genes from *N. nambi* were codon optimized for expression in *N. tabacum* and ordered synthetically from Evrogen. Synthetic genes were flanked by BsaI restriction sites designed to leave AATG-GCTT overhangs, compatible with the existing modular cloning standard described in ref. [14]. Each gene was then cloned into Level 1-like vector, under the control of the constitutive 35S promoter from cauliflower mosaic virus and ocs terminator from *Agrobacterium tumefaciens*. These Level 1 plasmids were then digested by BpiI and assembled together into a Level 2-like backbone in the following order: *nnhisps-nnh3h-nnluz-nncph* or, in the case of *cph*-less version, *nnhisps-nnh3h-nnluz*. This gene cluster was preceded by a kanamycin resistance cassette for selection in plants. The entire construct, consisting of the kanamycin cassette plus luminescence genes, was flanked by *A. tumefaciens* insertion sequences to facilitate *Agrobacterium*-mediated random integration of the construct into plant genomes (Supplementary Fig. 2).

All clonings described above were performed according to established Golden Gate cloning methods, wherein digestion and ligation are performed together in a single step. All reactions were performed in 1× T4 ligase buffer (Thermo Fisher) containing 10 U of T4 ligase, 20 U of either BsaI or BpiI (Thermo Fisher) and 100 ng of DNA of each DNA part. Golden Gate reactions were performed according to "troubleshooting" cycling conditions described in ref. [15]: 25 cycles between 37 °C and 16 °C (90 s at 37 °C, 180 s at 16 °C) and then 5 min at 50 °C and 10 min at 80 °C.

Correct sequences of all plasmids were confirmed with Sanger and Illumina sequencing before use (Supplementary Data).

Assembly of plasmids for mammalian cells. DNA coding for RcTAL, HpaB, HpaC, nnHispS, NpgA, nnH3H, nnCPH and nnLuz was ordered synthetically (Evrogen) and cloned into the pKatushka2S-C1 vector (Evrogen) instead of Katushka2S coding sequence, under the control of CMV promoter. Plasmid sequences are available in Genbank under the following accession numbers: pHpaB-C1, MT233533; pHpaC-C1, MT233534; pnnCPH-C1, MT233535; pnnH3H-C1, MT233536; pnnHispS-C1, MT233537; pnnLuz-C1, MT233538; pnpgA-C1, MT233539; pRcTAL-C1, MT233540; pX037, MT233541. Correct sequences of all plasmids were confirmed with Sanger and Illumina sequencing before use (Supplementary Data).

Expression in cultured mammalian cells and luminescence imaging. HEK293T cell line was transfected with a mixture of all eight plasmids by FuGENE HD Transfection Reagent (Promega). Transfected cells were grown in DMEM (PanEco) supplemented with 10% fetal bovine serum (HyClone), 4 mM L-glutamine, 10 U ml^{-1} penicillin and 10 μg ml^{-1} streptomycin, at 37 °C, 5% CO_2. Twenty-four hours after transfection, the medium was changed to MEM supplemented with 20 mM HEPES, and luminescence was analyzed by IVIS Spectrum CT (PerkinElmer). For the analysis, the background luminescence signal from the empty wells was subtracted from the luminescence signal of wells with control and autoluminescent cells.

Agrobacterium-mediated transformation of plants. Assembled plasmids were transferred into *A. tumefaciens* strain AGL0 (ref. [16]). Bacteria were grown in flasks on a shaker overnight at 28 °C in LB medium supplemented with 25 mg l^{-1} rifampicin and 50 mg l^{-1} kanamycin. Bacterial cultures were diluted in liquid Murashige and Skoog (MS) medium to an optical density of 0.6 at 600 nm.

Leaf explants used for transformation experiments were cut from 2-week-old tobacco plants (*N. tabacum* cv. Petit Havana SR1, *N. benthamiana*) and incubated with bacterial culture for 20 min. Leaf explants were then placed onto filter paper overlaid on MS medium (MS salts, MS vitamin, 30 g l^{-1} sucrose, 8 g l^{-1} agar, pH 5.8) supplemented with 1 mg l^{-1} 6-benzylaminopurine and 0.1 mg l^{-1} indolyl acetic acid. Two days after inoculation, explants were transferred to the same medium supplemented with 500 mg l^{-1} cefotaxime and 75 mg l^{-1} kanamycin. Regeneration shoots were cut and grown on MS medium with antibiotics.

Molecular analysis of transgenic plants. Genomic DNA was extracted from young leaves of greenhouse-grown plantlets using the cetyltrimethylammonium bromide method[17]. The presence of each of the transferred genes was confirmed by PCR with gene-specific primers (Supplementary Table 2).

For Southern blots, 30 μg of plant genomic DNA was digested overnight at 37 °C by 100 U of EcoRV, a restriction enzyme that cuts T-DNA constructs used in this study at a single position inside the nnHispS coding region. After gel electrophoresis, digestion products were transferred onto Amersham Hybond-N+ membrane (GE Healthcare) and immobilized. The DNA probe was constructed by PCR using cloned synthetic *nnluz* gene as the template and *nnluz*-specific primers listed in Supplementary Table 2. Probe DNA was labeled with alkaline phosphatase using the AlkPhos Direct Labeling Kit (GE Healthcare). Prehybridization, hybridization (overnight at 60 °C) with alkaline phosphatase-labeled probe and subsequent washings of the membrane were carried out according to the AlkPhos Direct Labeling Kit protocol. Detection was performed using Amersham CDP-Star detection reagent following the manufacturer's protocol (GE Healthcare). The signal from the membrane was accumulated on X-ray film (XBE blue sensitive, Retina) in film cassette at room temperature for 24 h. X-ray films were scanned on an Amersham Imager 600 (GE Healthcare Life Sciences).

Plant growth conditions. Plant transgenesis and cultivation were carried out at the artificial climate station Biotron N2-2.9 (branch of the Shemyakin-Ovchinnikov Institute of Bioorganic Chemistry of the Russian Academy of Sciences). Tobacco plants were propagated on MS medium supplemented with 30 g l^{-1} sucrose and 0.8 wt/vol agar (Panreac). In vitro cultures were incubated at 24 ± 1 °C with a 12–16-d photoperiod, with mixed cool white and red light (Cool White and Gro-Lux fluorescent lamps) at a light intensity of 40 μmol s^{-1} m^{-2}. After root development, plantlets were transferred to 9-cm pots with sterilized soil (1:3 wt/wt mixture of sand and peat). Potted plants were placed in the greenhouse at 22 ± 2 °C under neutral day conditions (12 h light/12 h dark; 150 μmol s^{-1} m^{-2}) and 75% relative humidity. For time-lapse imaging of germinating seeds (Supplementary Video 2), seeds were sterilized in sodium hypochlorite (25%/15 min) and then propagated on MS medium supplemented with 30 g l^{-1} sucrose and 0.3 wt/vol Gellan Gum Powder (MP Biomedicals). The same medium was used for luminescence imaging of roots (Fig. 2d and Supplementary Videos 3 and 4).

Plant imaging setup with photo cameras. We used a Sony Alpha ILCE-7M3 camera to capture all photos and videos presented in this article, except those taken on a smartphone (Supplementary Fig. 8) and a long-term time lapse filmed on a Nikon D800 camera (Supplementary Video 5). Depending on the experimental setup, lens aperture and other considerations, a range of ISO values from 3,200 to 40,000 was used, with exposure times from 5 s (leaf injury) to 20 min (root microscopy). Most of the photos were captured with a 30-s exposure time.

We used an SEL50M28 lens (Sony, f/2.8) or a 35-mm T1.5 ED AS UMC VDSLR lens (Samyang, ~f/1.4). Long-term time lapse of growing tobacco plants (Supplementary Fig. 13c and Supplementary Video 5) was captured with a Nikon D800 camera and a Sigma AF 35-mm f/1.4 DG HSM Art at ISO 8063 and 30-s shutter speed. Root microscopy was performed with a Sony Alpha ILCE-7M3 camera with Meiji MA833 U. A Plan 20× objective lens was mounted on the camera via a custom-made adaptor. For quantitative comparison, XLS-4 (PerkinElmer) calibrated light source was used as a reference (emits 1.6×10^9 photons per second at 525 nm).

The photos were then processed in the following way. First, a raw photo obtained in the dark with the same settings was per-channel subtracted from a raw photo of plants (LibRaw version 0.19.2, 4channels tool) to remove hot pixels and reduce noise. Optionally, an ImageJ plugin was applied (https://imagej.nih.gov/ij/source/ij/plugin/filter/RankFilters.java) to remove outliers (hot pixels). For most photos, only the green channels (G and G2) were kept in the final image. Final images were rendered in pseudocolor with either "Green" or "Fire" linear lookup tables from ImageJ.

Plant imaging on IVIS Spectrum CT. Plant imaging on IVIS Spectrum CT was performed without filters in front of the camera, with 1-min exposure and without binning. The samples were acquired with "C" settings of field of view. Ambient light image was taken after the luminescence measurements. Other settings were left at defaults.

Chlorophyll content in leaves. Next, 0.5 g of fresh plant leaf sample was homogenized in tissue homogenizer with 10 ml of 95% ethanol. Homogenized sample mixture was centrifuged at 10,000 r.p.m. for 15 min. An aliquot of the supernatant (0.5 ml) was mixed with 95% ethanol (4.5 ml). The solution mixture in a glass cuvette was analyzed for chlorophyll-a, chlorophyll-b and carotenoids content at 664, 649 and 470 nm.

Plant imaging on a smartphone. We used a Huawei P30 Pro smartphone for photography. To capture the photo displayed on Supplementary Fig. 8b, we used the following settings: 30-s exposure time, ISO 6400 and aperture 1.6.

Absorption spectra of tobacco leaves. The leaves from adult wild-type *N. tabacum* plants were collected and measured directly by spectrophotometer (Cary 100 Bio, Varian).

Imaging of leaf injuries. Plants were cultivated in a greenhouse for 6 weeks. Leaves of *N. tabacum* were wounded with a blade, causing a cut across the midvein.

Treatment with methyl jasmonate. Three-week-old transgenic bioluminescent *N. tabacum* plants were treated with methyl jasmonate (5 mM in 10 mM MES buffer, pH 7.0) by spraying. Control plants were treated with buffer (10 mM MES buffer, pH 7.0). Plants were then imaged in closed glass jars for 3 d in the dark.

Incubation with banana skin. Three-week-old transgenic bioluminescent *N. tabacum* plants were imaged with ripe banana skin in closed glass jars for 24 h.

Quantitative PCR. In experiments aimed to determine whether expression of *nnluz* gene oscillates during the day, we collected the third leaf counting from the apical bud from 27 25-day-old transgenic glowing plants. The leaves were collected with 3-h intervals during 24 h, and leaves from three plants were collected at each time point. From each plant, we collected leaves only once. All leaves were flash frozen in liquid nitrogen and homogenized for RNA extraction with TRIzol kit (Thermo Fisher Scientific). Synthesis of the first cDNA strand was carried out with an MMLV kit (Evrogen). Quantitative PCR was performed with qPCRmix-HS SYBR + LowROX kit (Evrogen) on a 7500 Real-Time PCR machine (Applied Biosystems) with primers annealing at the *nnluz* transcript: GGACCAGGAGTCCCAGGC and CTTGGCATTTTCGACAATCTTA with the following program: 95 °C for 1 min and then 40 cycles of 95 °C for 15 s, 60 °C for 15 s and 72 °C for 15 s.

Infiltration of tobacco leaves with hispidin precursors. For experiments with infiltration of transgenic *N. benthamiana* leaves, we prepared 100 uM solutions of caffeic acid, malonyl-CoA, ATP and coenzyme A in 10 mM MES buffer (pH 7.0). We also prepared 100 uM mixtures of these compounds in the same buffer: Mix 1, full (caffeic acid, malonyl-CoA, CoA, ATP); Mix 2 without caffeic acid (malonyl-CoA, CoA, ATP); Mix 3 without malonyl-CoA (caffeic acid, CoA, ATP); Mix 4 without CoA (caffeic acid, malonyl-CoA, ATP); and Mix 5 without ATP (caffeic acid, malonyl-CoA, CoA). The solutions were injected into the blades of cut *N. benthamiana* leaves, and leaves were imaged for 15 min after injections. The analysis of the frame at 1 min after injection is presented in Supplementary Fig. 9. Similar experiment design was followed for the injection of luciferin precursors into *N. tabacum* leaves, followed by 16 h of imaging (Supplementary Video 1).

LC-MS/MS analysis. Analytical standard (≥ 98.0) caffeic acid and acetic acid were purchased from Sigma-Aldrich. Hispidin was synthesized by Planta (≥ 95.0%). HPLC-grade acetonitrile was purchased from J.T. Baker. Deionized water was obtained from a Milli-Q System.

We analyzed several groups of samples: leaves and flowers of the wild-type *N. tabacum* (NT000) and two transgenic lines of plants (NT001 and NT078). Immediately after collection, the samples were frozen in liquid nitrogen and manually ground in a mortar. To reduce biological variability, we mixed plant material from three different organisms of the same group. For each sample, about 1 g of the frozen tissue was lyophilized in 50-ml Falcon tubes, and freeze-dried material was stored at −20 °C. Each sample was prepared and analyzed in three replicates.

For the analysis, about 50 mg of lyophilized powder was weighed and treated with 7 ml of 70% methanol for 30 min in an ultrasonic bath and then centrifuged for 10 min at 4,000 r.p.m. The supernatant was collected, filtered with Phenex GF/PVDF syringe filter (diameter 30 mm, pore size 0.45 µm) and analyzed on an LCMS instrument. Analyses were performed by a Shimadzu 8030 system consisting of HPLC coupled to PDA and triple quadrupole mass spectrometer (HPLC-DAD-ESI-TQ MS). The chromatographic separation was performed on Discovery C18 column 4.6 × 150 mm, 5 µm in a gradient mode with mobile phase components A (0.3% acetic acid in water) and B (acetonitrile). The gradient run was performed in the following way: 0–4 min 10–40% B, 4–5 min 40–80%, 5–10.5 min, isocratic elution with 100% B and then returned to the initial condition. The column temperature was 40 °C, the flow rate was 1 ml min^{-1} and the sample injection volume was 20 µl.

The electrospray ionization (ESI) source was set in negative ionization mode. Multiple reaction monitoring was used to perform mass spectrometric quantification. MS conditions: interface voltage 3,500 V (ESI^-), nebulizer gas (nitrogen) flow 2.5 l min^{-1}, drying gas (nitrogen) flow 15 l min^{-1}, CID gas pressure 60 kPa, DL temperature 250 °C and heat block temperature 400 °C. High-purity argon was used as collision gas. The precursor and product ions (*m/z*) of target analytes were 178.95 and 134.95 for caffeic acid and 245.05 and 159.00 for hispidin; collision energy was 35 V for both compounds.

Owing to the lack of isotope-labeled standards, we added standards to samples to account for substantial matrix effect. Each sample was analyzed twice, with and without the addition of standards. After the first analysis, a solution with a known amount of caffeic acid and hispidin was added. Assuming a linear relation between the observed signal and concentration of compounds, concentration of the extract was calculated as $C_{extr} = C_{ad} \times S_{extr}/(S_{tot} - S_{extr})$, where C_{ad} is concentration of the added compound in the extract and S_{extr} and S_{tot} are the analyte peak area in the first and second analyses.

Statistics. Data are plotted as box plots implemented in Seaborn (https://seaborn.pydata.org/) package (version 0.10, Python version 3.6). The boxes extend from the lower to upper quartile values of the data, and the horizontal line represents the median. Whiskers represent the full data range. Two-tailed Mann–Whitney *U* tests (Supplementary Fig. 3) were computed with the scipy.stats package (https://www.scipy.org/, SciPy version 1.3.1). The Scikit-posthocs Python package (https://pypi.org/project/scikit-posthocs/, version 0.6.2) was used for multiple pairwise post hoc Mann–Whitney *U* tests with *P* values corrected by the step-down method using Sidak adjustments (Supplementary Fig. 9). Sample numbers (*n*), statistical tests used and exact *P* values can be found in the figure legends.

Reporting Summary. Further information on research design is available in the Nature Research Reporting Summary linked to this article.

Data availability

The data sets generated or analyzed in the current study are available from the corresponding authors upon reasonable request. Unprocessed images of luminescent flowers captured on a Sony Alpha ILCE-7M3 camera and IVIS Spectrum CT are available from Figshare (https://doi.org/10.6084/m9.figshare.11353601). Plasmid sequences are available in Genbank under the following accession numbers: pHpaB-C1, MT233533; pHpaC-C1, MT233534; pnnCPH-C1, MT233535; pnnH3H-C1, MT233536; pnnHispS-C1, MT233537; pnnLuz-C1, MT233538; pnpgA-C1, MT233539; pRcTAL-C1, MT233540; pX037, MT233541. Sanger and Illumina sequencing results are available as Supplementary Data.

References

14. Weber, E., Engler, C., Gruetzner, R., Werner, S. & Marillonnet, S. *PLoS ONE* **6**, e16765 (2011).
15. Iverson, S. V., Haddock, T. L., Beal, J. & Densmore, D. M. *ACS Synth. Biol.* **5**, 99–103 (2016).
16. Lazo, G. R., Stein, P. A. & Ludwig, R. A. *Biotechnology* **9**, 963–967 (1991).
17. Rogers, S. O. & Bendich, A. J. *Plant Molecular Biology Manual* (Springer, 1994).

Acknowledgements

This study was designed, performed and funded by Planta LLC. We thank K. Wood for assisting in manuscript development. Planta acknowledges support from the Skolkovo Innovation Centre. We thank D. Bolotin and the Milaboratory (milaboratory.com) for access to computing and storage infrastructure. We thank S. Shakhov for providing photography equipment. The Synthetic Biology Group is funded by the MRC London Institute of Medical Sciences (UKRI MC-A658-5QEA0, K.S.S.). K.S.S. is supported by an Imperial College Research Fellowship. Experiments were partially carried out using equipment provided by the Institute of Bioorganic Chemistry of the Russian Academy of Sciences Core Facility (CKP IBCH; supported by the Russian Ministry of Education and Science Grant RFMEFI62117X0018). The F.A.K. lab is supported by ERC grant agreement 771209—CharFL. This project received funding from the European Union's Horizon 2020 Research and Innovation Programme under Marie Skłodowska-Curie Grant Agreement 665385. K.S.S. acknowledges support by President's Grant 075-15-2019-411. Design and assembly of some of the plasmids was supported by Russian Science Foundation grant 19-74-10102. Imaging experiments were partially supported by Russian Science Foundation grant 17-14-01169p. LC-MS/MS analyses of extracts were supported by Russian Science Foundation grant 16-14-00052p. Design and assembly of plasmids was partially supported by grant 075-15-2019-1789 from the Ministry of Science and Higher Education of the Russian Federation allocated to the Center for Precision Genome Editing and Genetic Technologies for Biomedicine. The authors would like to acknowledge the work of Genomics Core Facility of the Skolkovo Institute of Science and Technology, which performed the sequencing and bioinformatic analysis.

Author contributions

T.M., A.S.M., L.G.S., T.V.C., E.B.G., T.A.K., N.M.M., S.V.C., A.S.T., L.I.F., K.A.P., E.S.S., Y.V.G., V.V.N., S.A.D., P.V.S., O.A.M., V.O.S., S.M.D., A.I.B., A.S.P. and K.S.S. performed experiments. T.M., A.S.M., L.G.S., T.V.C., E.B.G., T.A.K., N.M.M., S.V.C., A.S.T., L.I.F., K.A.P., E.S.S., Y.V.G., V.V.N., S.A.D., P.V.S., O.A.M., V.O.S., S.M.D., A.I.B., A.S.P., V.V.C., S.V.D., F.A.K., I.V.Y. and K.S.S. performed data analysis. A.S.M. designed imaging setup, planned and performed experiments, analyzed data and wrote the paper. I.V.Y. and K.S.S. proposed and directed the study, planned experimentation and wrote the paper. All authors reviewed and commented on the paper draft.

Competing interests

This work was supported by Planta LLC. I.V.Y. and K.S.S. are shareholders and employees of Planta. Planta has filed patent applications related to use of components of the fungal bioluminescent system and development of glowing transgenic organisms.

Additional information

Supplementary information is available for this paper at https://doi.org/10.1038/s41587-020-0500-9.

Correspondence and requests for materials should be addressed to I.V.Y. or K.S.S.

Reprints and permissions information is available at www.nature.com/reprints.

nature research

Corresponding author(s): Karen Sarkisyan, Ilia Yampolsky

Last updated by author(s): Feb 22, 2020

Reporting Summary

Nature Research wishes to improve the reproducibility of the work that we publish. This form provides structure for consistency and transparency in reporting. For further information on Nature Research policies, see Authors & Referees and the Editorial Policy Checklist.

Statistics

For all statistical analyses, confirm that the following items are present in the figure legend, table legend, main text, or Methods section.

n/a	Confirmed	
☐	☒	The exact sample size (*n*) for each experimental group/condition, given as a discrete number and unit of measurement
☐	☒	A statement on whether measurements were taken from distinct samples or whether the same sample was measured repeatedly
☐	☒	The statistical test(s) used AND whether they are one- or two-sided *Only common tests should be described solely by name; describe more complex techniques in the Methods section.*
☒	☐	A description of all covariates tested
☐	☒	A description of any assumptions or corrections, such as tests of normality and adjustment for multiple comparisons
☐	☒	A full description of the statistical parameters including central tendency (e.g. means) or other basic estimates (e.g. regression coefficient) AND variation (e.g. standard deviation) or associated estimates of uncertainty (e.g. confidence intervals)
☐	☒	For null hypothesis testing, the test statistic (e.g. *F*, *t*, *r*) with confidence intervals, effect sizes, degrees of freedom and *P* value noted *Give P values as exact values whenever suitable.*
☒	☐	For Bayesian analysis, information on the choice of priors and Markov chain Monte Carlo settings
☒	☐	For hierarchical and complex designs, identification of the appropriate level for tests and full reporting of outcomes
☒	☐	Estimates of effect sizes (e.g. Cohen's *d*, Pearson's *r*), indicating how they were calculated

Our web collection on statistics for biologists contains articles on many of the points above.

Software and code

Policy information about availability of computer code

Data collection	Python code for automated image acquisition
Data analysis	LibRaw version 0.19.2, 4channels command line tool, ImageJ plugin RankFilters, custom Python code for image and data processing, Seaborn (https://seaborn.pydata.org/) package, scipy.stats package (https://www.scipy.org/). Scikit-posthocs Python package (https://pypi.org/project/scikit-posthocs/) for statistical analysis

For manuscripts utilizing custom algorithms or software that are central to the research but not yet described in published literature, software must be made available to editors/reviewers. We strongly encourage code deposition in a community repository (e.g. GitHub). See the Nature Research guidelines for submitting code & software for further information.

Data

Policy information about availability of data

All manuscripts must include a data availability statement. This statement should provide the following information, where applicable:

- Accession codes, unique identifiers, or web links for publicly available datasets
- A list of figures that have associated raw data
- A description of any restrictions on data availability

The datasets generated or analysed during the current study are available from the corresponding authors on reasonable request.

Field-specific reporting

Please select the one below that is the best fit for your research. If you are not sure, read the appropriate sections before making your selection.

☒ Life sciences ☐ Behavioural & social sciences ☐ Ecological, evolutionary & environmental sciences

For a reference copy of the document with all sections, see nature.com/documents/nr-reporting-summary-flat.pdf

Life sciences study design

All studies must disclose on these points even when the disclosure is negative.

Sample size	The experiments described in this study were done for the first time. Due to exploratory nature of our study we refrained from unnecessary generalizations. No pre-specified effect size could be determined a priori. In cases of assessment of the effect of external stimuli on transgenic plants, and in the case of determination of chemical composition of plant samples, the sample size were selected in accordance with the standards in the field.
Data exclusions	No data were excluded from the study.
Replication	Number of replicates are explicitly stated in the figure legends. Where applicable, reported results were consistently replicated across multiple experiments with all replicates generating similar results.
Randomization	Randomization is not relevant to our study design because investigators were comparing plant samples under well controlled conditions. No human or animal subjects were used in the study.
Blinding	No blinding was performed as there was no animal or human groups.

Reporting for specific materials, systems and methods

We require information from authors about some types of materials, experimental systems and methods used in many studies. Here, indicate whether each material, system or method listed is relevant to your study. If you are not sure if a list item applies to your research, read the appropriate section before selecting a response.

Materials & experimental systems

n/a	Involved in the study
☒	☐ Antibodies
☐	☒ Eukaryotic cell lines
☒	☐ Palaeontology
☒	☐ Animals and other organisms
☒	☐ Human research participants
☒	☐ Clinical data

Methods

n/a	Involved in the study
☒	☐ ChIP-seq
☒	☐ Flow cytometry
☒	☐ MRI-based neuroimaging

Eukaryotic cell lines

Policy information about cell lines

Cell line source(s)	HEK293T (unknown origin)
Authentication	Cell line was authenticated morphologically.
Mycoplasma contamination	Cell lines were frequently tested for mycoplasma contamination. Cell line used in this study was verified to be mycoplasma negative before undertaking experiments with it.
Commonly misidentified lines (See ICLAC register)	No commonly misidentified cells were used. All cells displayed homogeneous characteristic morphology.